Electronic Supplementary Material (ESI) for RSC Advances.


# Preparation of novel bridged bis(β-cyclodextrin) chiral stationary phase by thiol-ene click chemistry for enhanced enantioseparation in HPLC

Ning Zhang, Siyu Guo and Bolin Gong*

School of Chemistry and Chemical Engineering, North Minzu University, Yinchuan 750021, China.

*Prof. Bolin Gong

No. 204 Wenchang North Street, Xixia District, Yinchuan City, China

E-mail: gongbolin@163.com

## Figure captions

Fig. S1. The mass spectra of allyl-ureido-β-CD (a) and bridged bis (β-CD) ligand (b).

Fig. S2. The $^{1}$HNMR spectrum of the bridged bis(β-CD) ligand.

Fig. S3. The infrared spectra of the bridged bis(β-CD) ligand (a) and HTCDP (b).

Fig. S4. The thermogravimetric analysis of HTCDP.

Fig. S5. Scanning electron microscopy (SEM) of HTCDP.

Fig. S6. Solid state 13C NMR of HTCDP. 105–65 ppm: C atoms on CD glucose unit.

Fig. S7. The chemical structures of 8 flavanones.

Fig. S8. The chemical structures of 8 triazole pesticides.

Fig. S9. The chemical structures of myclobutanil, ornidazole, voriconazole and lansoprazole.

Fig. S10. The chemical structures of 5 common chiral compounds.

Fig.S11. The effect of column temperature on the resolution, separation factor and retention factor of flavanones.

Fig.S12. The effect of column temperature on the resolution, separation factor and retention factor of triazole pesticides.

## Table captions

Table S1. The elemental analysis results of HTCDP and CDCSP.

Table S2. The effect of mobile phase type on 2-Hydroxyflavanone and 4-Hydroxyflavanone.

Table S3. Separation data of 2-hydroxyflavanone at different temperatures.

Table S4. The separation results and optimal separation conditions of myclobutanil, ornidazole, voriconazole and lansoprazole on HTCDP.

Table S5. Separation data of Hexaconazole at different temperatures.

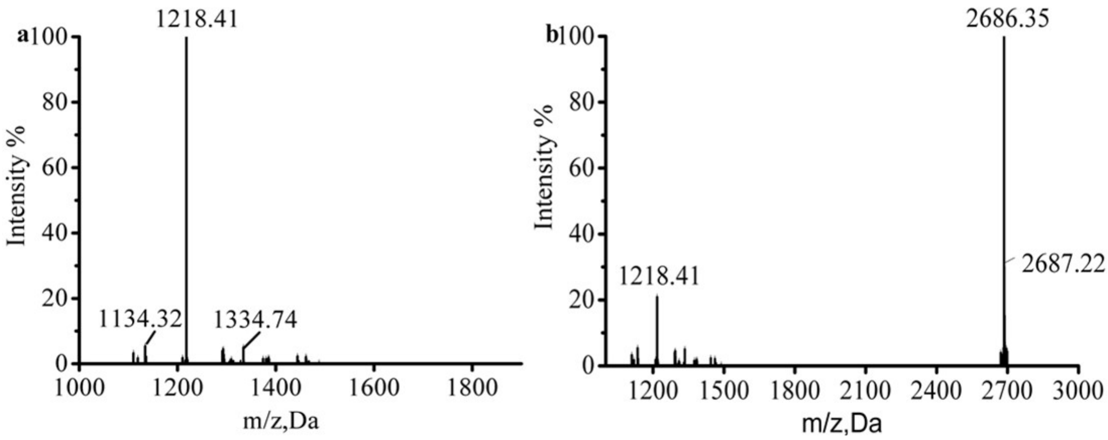


Fig. S1. The mass spectra of allyl-ureido-β-CD (a) and bridged bis (β-CD) ligand (b)

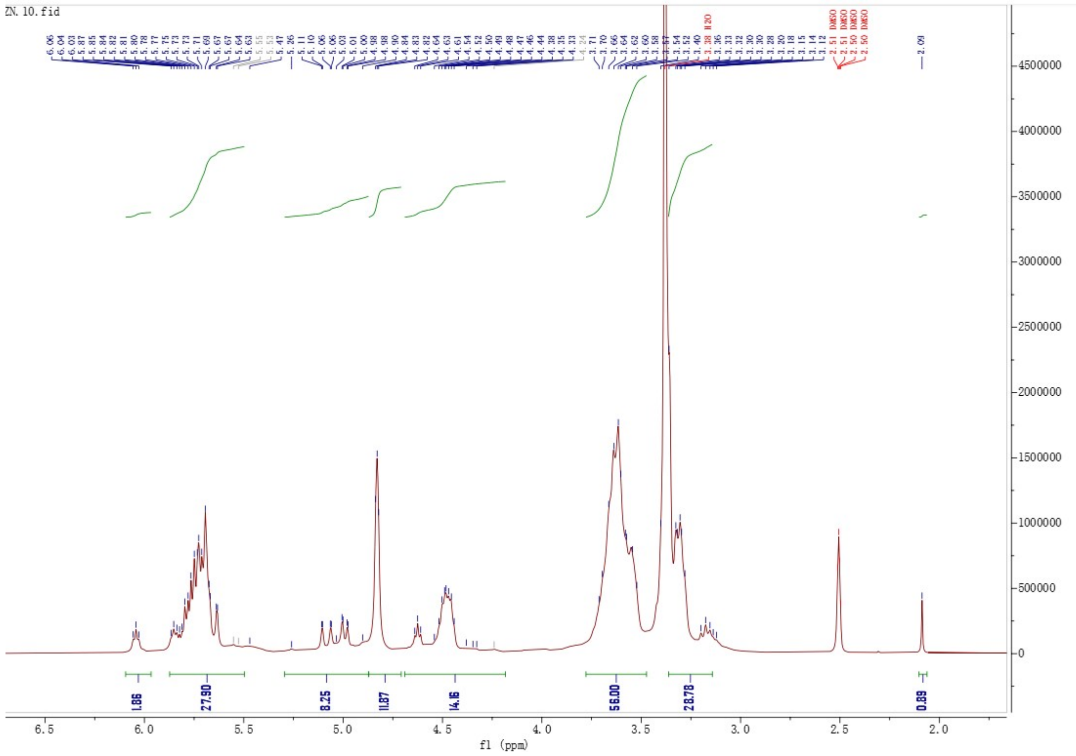

Fig. S2. The $^{1}$HNMR spectrum of the bridged bis(β-CD) ligand

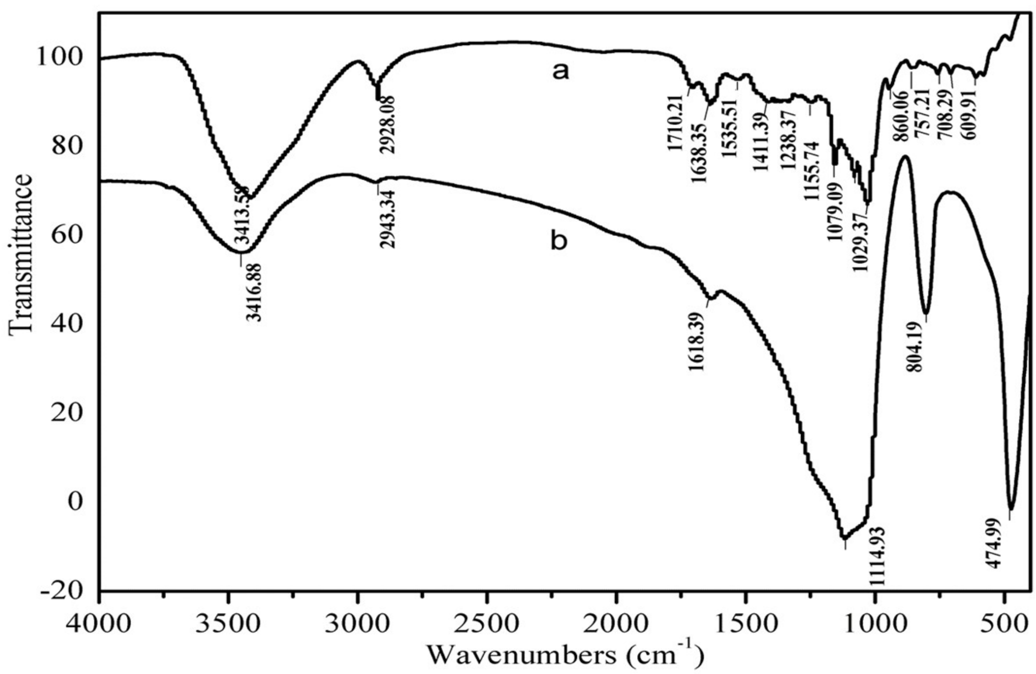


Fig. S3. The infrared spectra of the bridged bis(β-CD) ligand (a) and HTCDP (b)

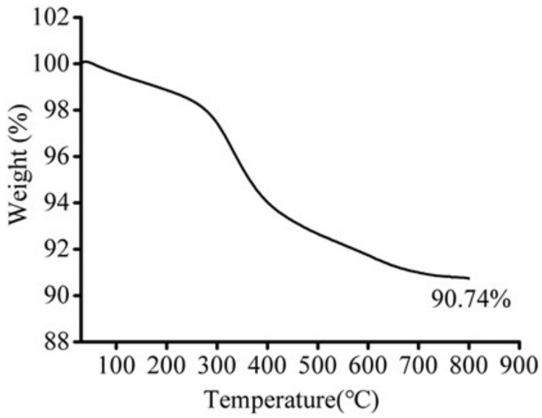


Fig. S4. The thermogravimetric analysis of HTCDP

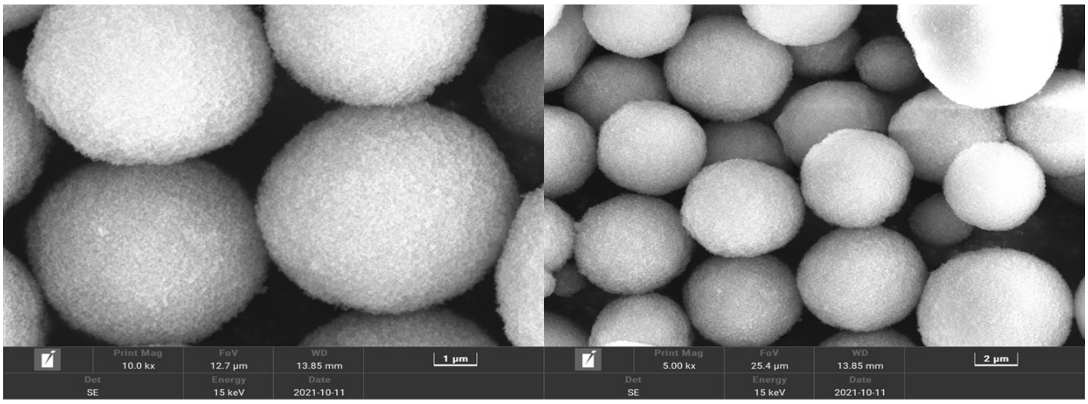


Fig. S5. Scanning electron microscopy (SEM) of HTCDP

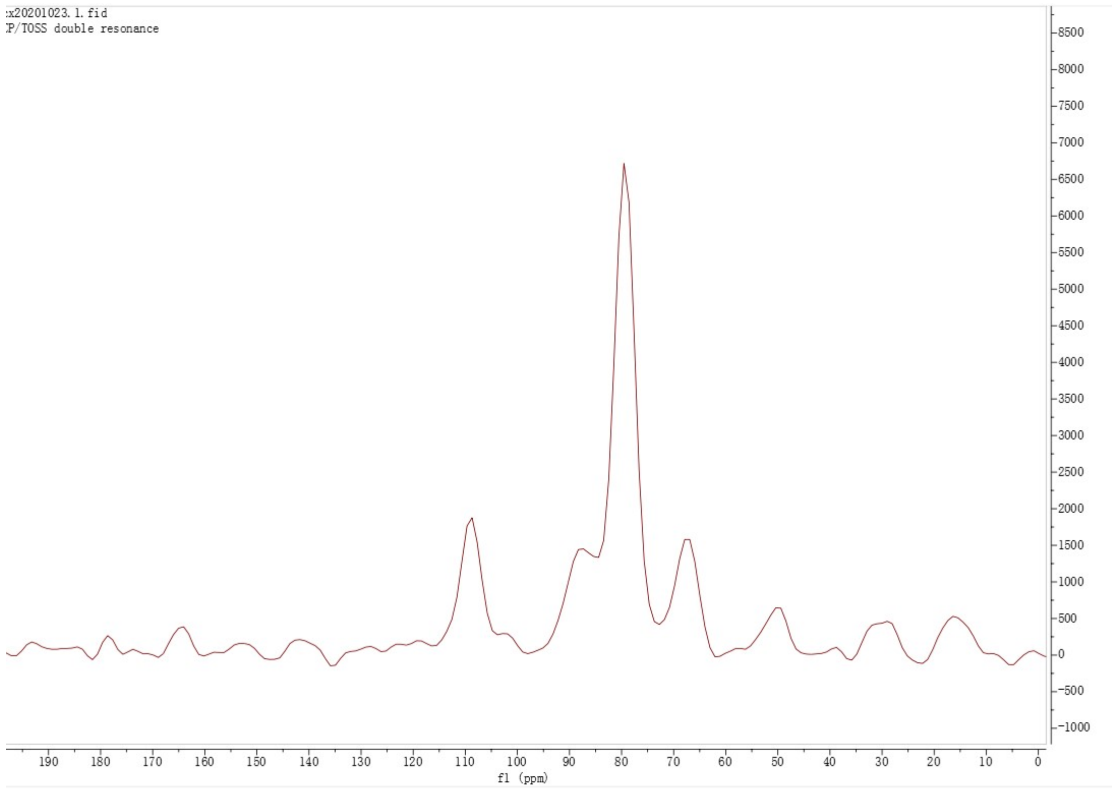


Fig. S6. Solid state 13C NMR of HTCDP. 105–65 ppm: C atoms on CD glucose unit

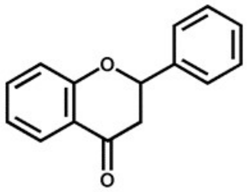

**Flavanone**

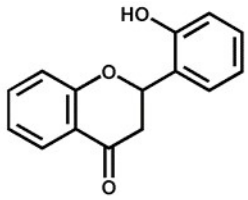

**2'-Hydroxy Flavanone**

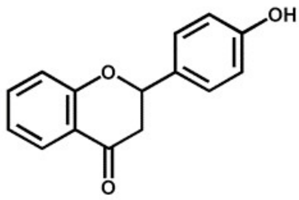

**4'-Hydroxy Flavanone**

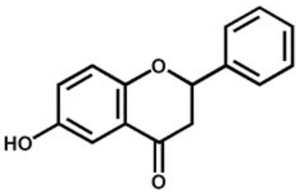

**6-Hydroxy Flavanone**

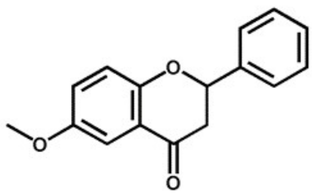

**6-Methoxy Flavanone**

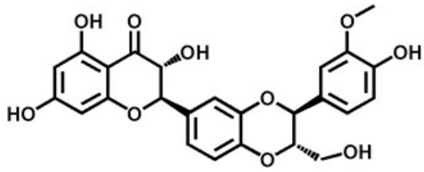

**Silymarin A/B**

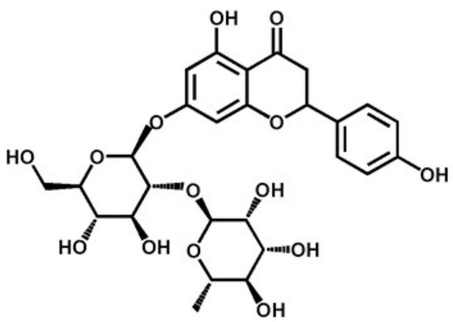

**Naringin**

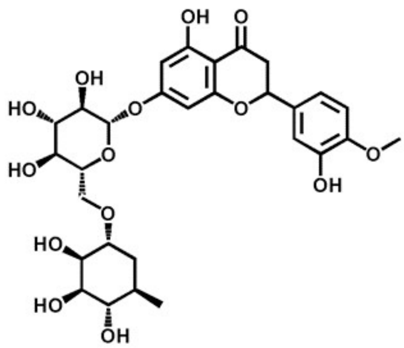

**Hesperidin**

Fig. S7. The chemical structures of 8 common flavanones

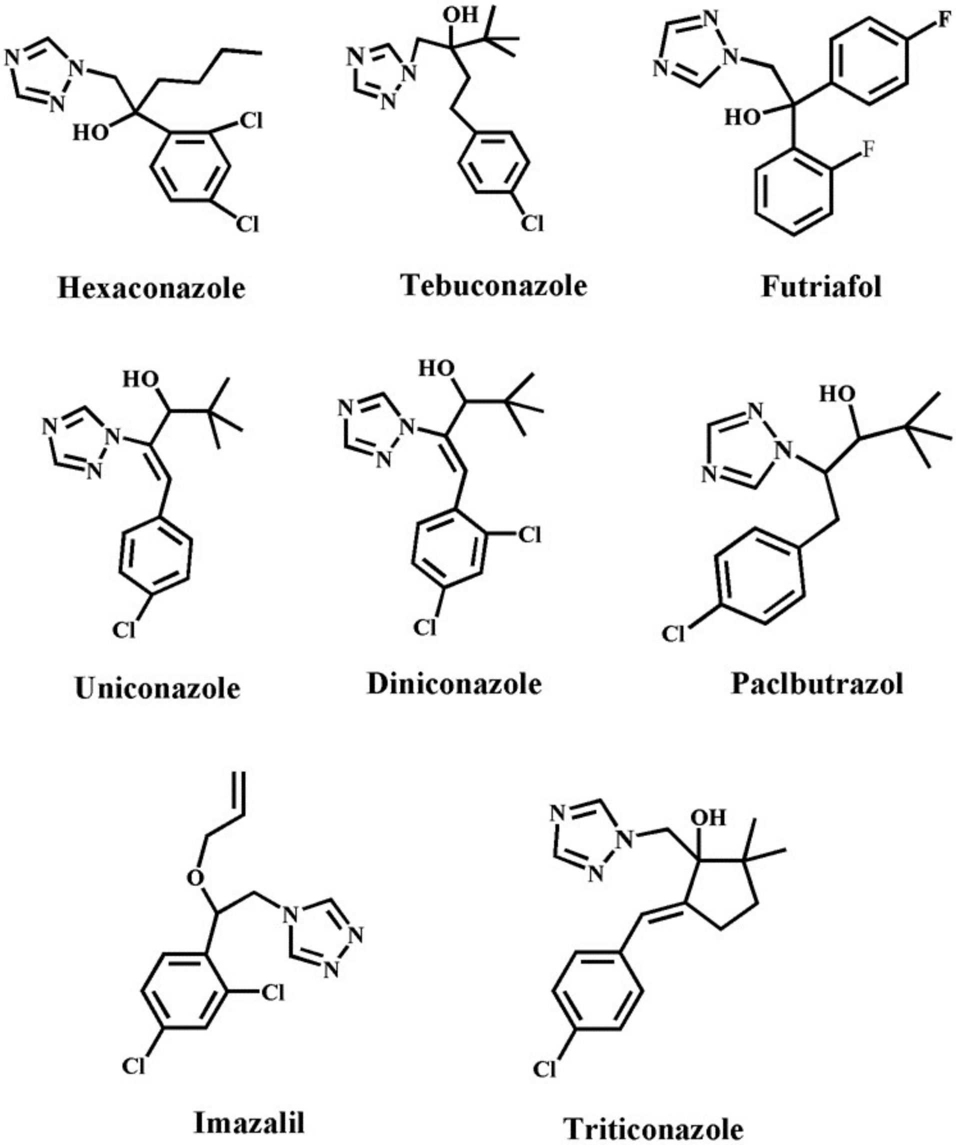


Fig. S8. The chemical structure of 8 triazole pesticides

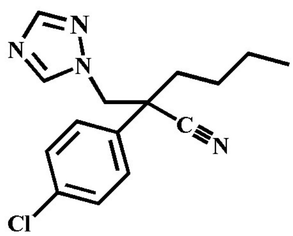

**Myclobutanil**

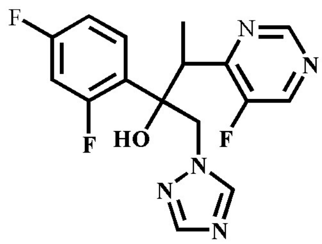

**Voriconazole**

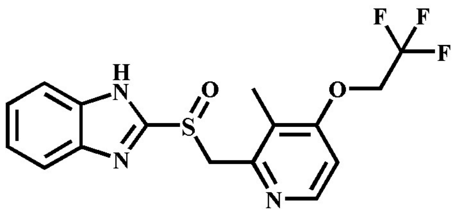

**Lansoprazole**

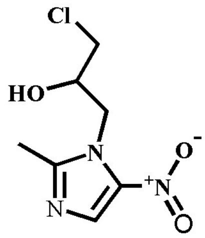

**Ornidazole**

Fig. S9. The chemical structures of myclobutanil, ornidazole, voriconazole and lansoprazole

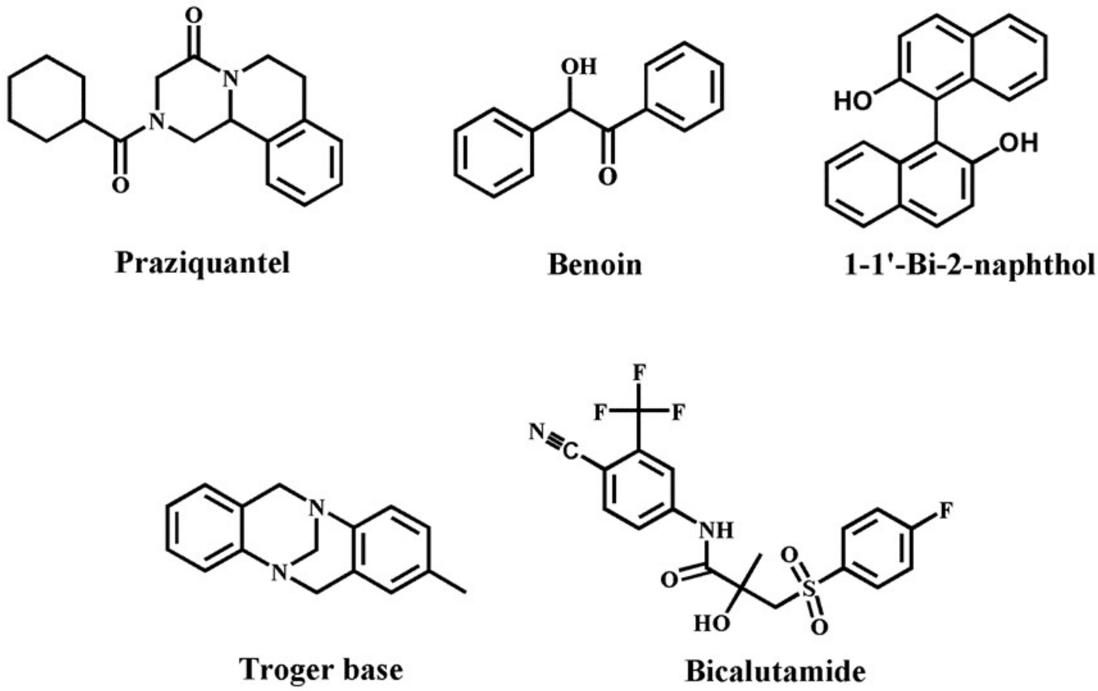


Fig. S10. The chemical structures of 5 common chiral compounds

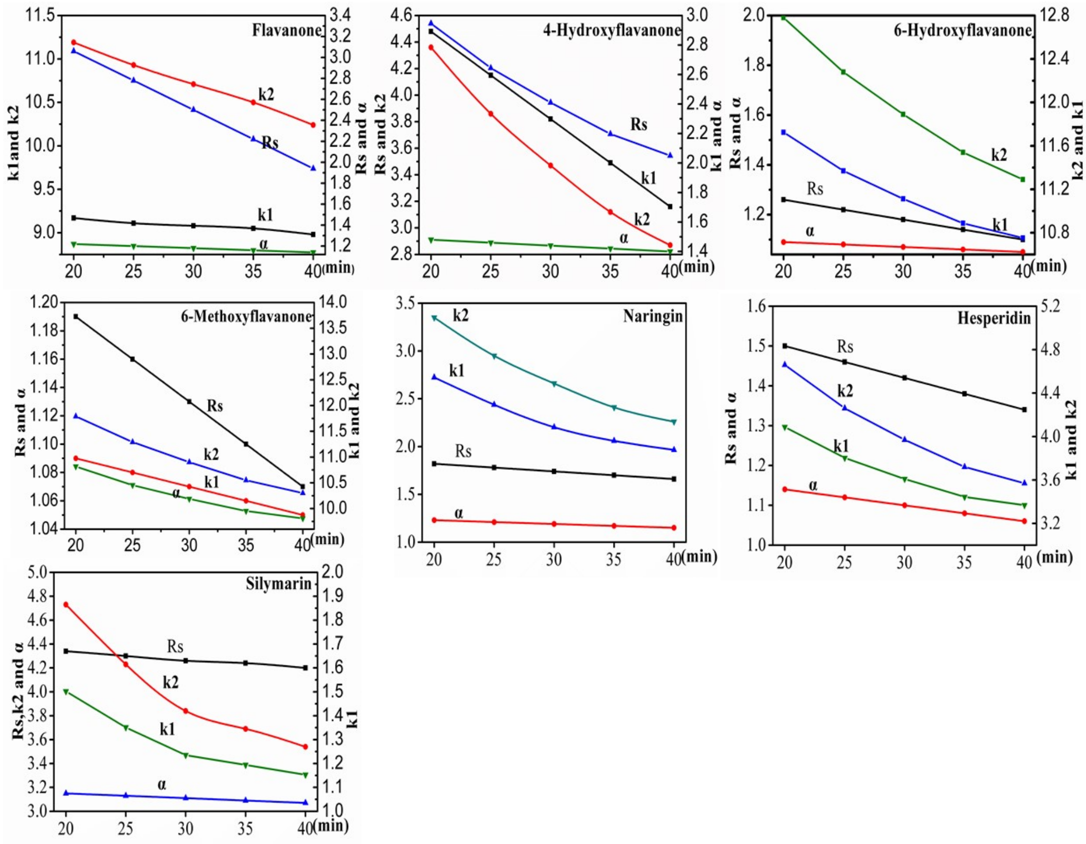


Fig. S11. The effect of column temperature on the resolution, separation factor and retention factor of flavanones

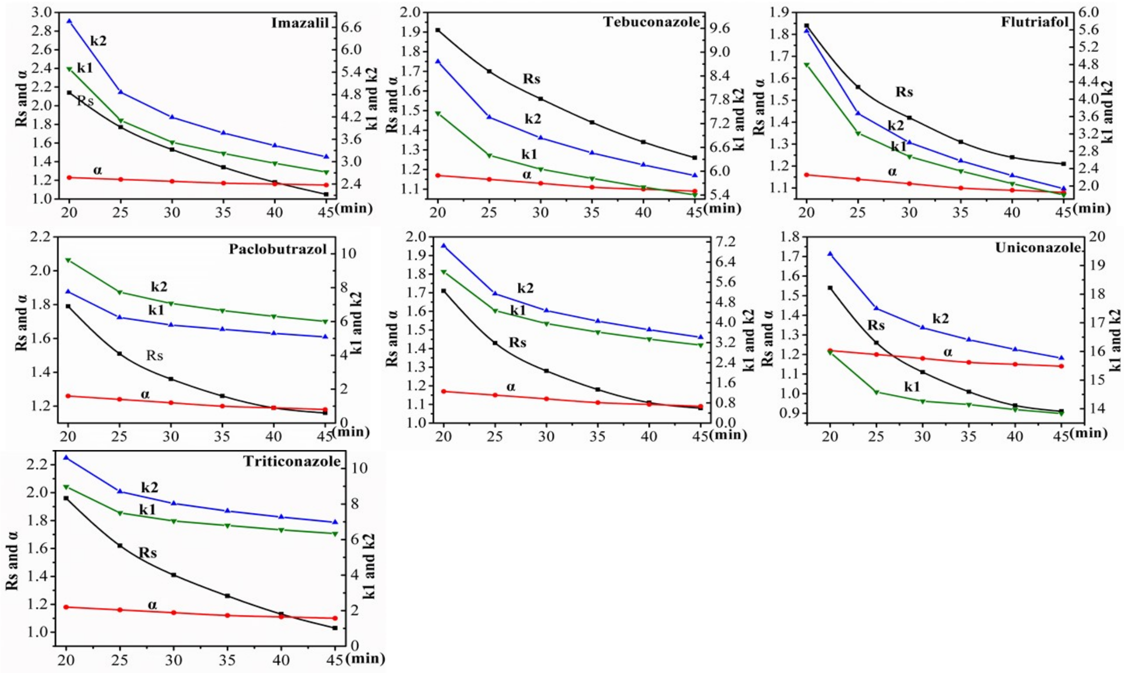


Fig. S12. The effect of column temperature on the resolution, separation factor and retention factor of triazole pesticides

Table S1. The elemental analysis results of HTCDP and CDCSP.

| CSPs | C % | H % | N % | S % | Surface loading |
|---|---|---|---|---|---|
| HTCDP | 3.23 | 0.46 | 0.24 | 0.12 | 0.45 μmol/$m^2$ |
| CDCSP | 1.60 | 0.28 | 0.38 | / | 0.51 μmol/$m^2$ |

Table S2. The effect of mobile phase type on 2-Hydroxyflavanone and 4-Hydroxyflavanone

| Compounds | $k_1$ | $k_2$ | α | Rs | Mobile phases(v/v) | Temp (℃) | CSPs |
|---|---|---|---|---|---|---|---|
| 2-Hydroxy | 2.11 | 2.96 | 1.40 | 3.39 | ACN/0.1%FA (20/80) | 20 | HTCDP |
| flavanone | 1.98 | 2.56 | 1.29 | 2.06 | MeOH/0.1%FA (20/80) | 20 | HTCDP |
| 4-Hydroxy | 2.94 | 4.36 | 1.48 | 4.48 | ACN/0.1%FA (20/80) | 20 | HTCDP |
| flavanone | 2.76 | 3.61 | 1.31 | 2.68 | MeOH/0.1%FA (20/80) | 20 | HTCDP |

Table S3. Separation data of 2-hydroxyflavanone at different temperatures

| | Rs | $k_1$ | $k_2$ | α |
|---|---|---|---|---|
| 20 °C | 3.89 | 2.11 | 2.96 | 1.40 |
| 25 °C | 3.56 | 1.78 | 2.46 | 1.38 |
| 30 °C | 3.24 | 1.52 | 2.07 | 1.36 |
| 35 °C | 2.91 | 1.28 | 1.72 | 1.34 |
| 40 °C | 2.58 | 1.11 | 1.47 | 1.32 |

Table S4. The separation results and optimal separation conditions of myclobutanil, ornidazole, voriconazole and lansoprazole on HTCDP

| No. | Compounds | $k_1$ | $k_2$ | α | Rs | Mobile phases(v/v) | Temp (℃) | CSPs |
|---|---|---|---|---|---|---|---|---|
| 1 | Myclobutanil | 4.38 | 4.75 | 1.08 | <0.5 | ACN/$H_2O$ (10/90) | 20 | HTCDP |
| 2 | Ornidazole | 0.29 | / | / | / | ACN/$H_2O$ (10/90) | 20 | HTCDP |
| 3 | Voriconazole | 2.14 | / | / | / | ACN/$H_2O$ (10/90) | 20 | HTCDP |
| 4 | Lansoprazole | 2.21 | / | / | / | ACN/$H_2O$ (15/85) | 20 | HTCDP |

Note: k', retention factor; α, separation factor; Rs, resolution; Temp, temperature (℃); CSPs, chiral stationary phase; HTCDP, a novel bridged bis(β-cyclodextrin) chiral stationary phase; CDCSP, native β-cyclodextrin chiral stationary phase; /, no separation.

Table S5. Separation data of Hexaconazole at different temperatures

| | Rs | $k_1$ | $k_2$ | α |
|---|---|---|---|---|
| 20°C | 2.19 | 4.48 | 5.42 | 1.21 |
| 25°C | 1.82 | 2.96 | 3.52 | 1.19 |
| 30°C | 1.58 | 2.43 | 2.85 | 1.17 |
| 35°C | 1.39 | 2.11 | 2.43 | 1.15 |
| 40°C | 1.23 | 1.83 | 2.09 | 1.14 |
| 45°C | 1.10 | 1.59 | 1.79 | 1.13 |